Article

Subdiffraction Imaging through the Selective Donut-Mode Depletion of Thermally Stable Photoswitchable Fluorophores: Numerical Analysis and Application to the Fluorescent Protein Dronpa

Peter Dedecker, Jun-ichi Hotta, Cristina Flors, Michel Sliwa, Hiroshi Uji-i, Maarten B. J. Roeffaers, Ryoko Ando, Hideaki Mizuno, Atsushi Miyawaki, and Johan Hofkens

J. Am. Chem. Soc., **2007**, 129 (51), 16132-16141 • DOI: 10.1021/ja076128z

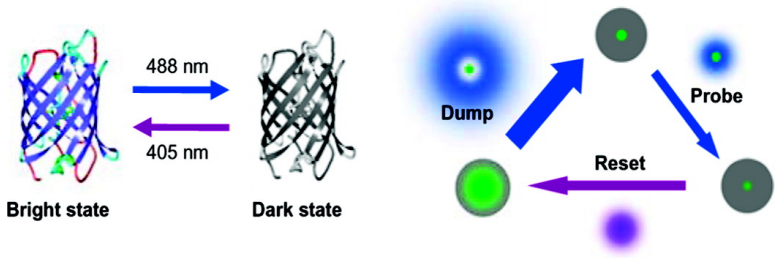

More About This Article

Additional resources and features associated with this article are available within the HTML version:

- Supporting Information
- Links to the 4 articles that cite this article, as of the time of this article download
- Access to high resolution figures
- Links to articles and content related to this article
- Copyright permission to reproduce figures and/or text from this article

View the Full Text HTML

J|A|C|S
ARTICLES
Published on Web 11/30/2007

Subdiffraction Imaging through the Selective Donut-Mode Depletion of Thermally Stable Photoswitchable Fluorophores: Numerical Analysis and Application to the Fluorescent Protein Dronpa

Peter Dedecker,[†] Jun-ichi Hotta,*[,†] Cristina Flors,[†] Michel Sliwa,[†] Hiroshi Uji-i,[†] Maarten B. J. Roeffaers,[†] Ryoko Ando,[‡] Hideaki Mizuno,[‡] Atsushi Miyawaki,[‡] and Johan Hofkens*[,†]

Contribution from the Department of Chemistry and INPAC, Katholieke Universiteit Leuven, Celestijnenlaan 200 F, 3001 Heverlee, Belgium, and Brain Science Institute, RIKEN, 2-1 Hirosawa, Wako, Saitama 351-0198, Japan

Received August 20, 2007; E-mail: johan.hofkens@chem.kuleuven.be; junichi.hotta@chem.kuleuven.be

Abstract: The fast and reversible on/off switching of the fluorescence emission of the GFP-like fluorescent protein Dronpa has attracted considerable interest for applications in subdiffraction imaging. In this paper we study the use of a donut-mode beam in combination with two more overlapping laser beams to increase the imaging resolution through selective switching to the nonfluorescent photoswitched state. We devise and run a series of numerical simulations to determine suitable photophysical parameters of prospective, thermally stable photoswitchable molecules, in terms of photoswitching quantum yields, fatigue resistance, and possible presence of transient nonfluorescent states. Many of our findings are applicable to other measurements that make use of donut beams, and these guidelines can be used in the synthesis and screening of novel photoswitchable compounds. We experimentally demonstrate the possibility of obtaining increased resolution by making use of the efficient and thermally stable Dronpa photoswitching, using equipment that is commonly available.

1. Introduction

In a relatively short amount of time fluorescence microscopy has evolved into a convenient and highly powerful tool for the imaging and study of key problems in the life sciences. This remarkable success can be attributed to the very high inherent sensitivity and selectivity of fluorescence detection, in combination with the relative noninvasiveness and convenience inherent to optical microscopy. As a result, a large variety of techniques for labeling target molecules and samples of interest has been developed, and in the past decades the field of optical labeling has been revolutionized by the discovery of the green fluorescent protein (GFP) and related proteins, which constitute a genetically encoded fluorescent marker.[1−3]

Unfortunately, even with the advent of these proteins fluorescence microscopy is not without its share of limitations. As with any microscopy technique, there is a lower limit to the sizes of the details that can be discerned, which is reflected in a finite spatial resolution. In modern-day fluorescence microscopes this finite resolution is a direct consequence of the wavelike character of light and is known as the diffraction limit, which is roughly 250 nm in many experiments. Unhindered by this limitation, living cells and tissues display a complex and elaborate ordering and structuring at length scales well below this limit. While this ordering is a fundamentally important concept, and highly interesting for or even crucial to present and future research efforts, it is thus seemingly inaccessible by direct optical means. Even though it can be revealed by other microscopic techniques, such as electron or scanning-probe microscopy, these approaches are usually limited by an elaborate and destructive sample preparation or measurement, or by an inability to visualize details beyond the surface of the sample.

Due to this limitation several schemes to achieve a resolution better than the diffraction limit in optical microscopy have been proposed or demonstrated.[4] One of the best-known approaches is stimulated-emission depletion (STED) microscopy.[5−7] STED relies on the realization of a carefully phase-modulated laser beam that is focused to obtain a "donut" mode at the focal point of the microscope, which is characterized by a sharp, zero-intensity "hole" at the center of the focus. Moreover, the wavelength of the donut-mode laser beam is chosen at the red edge of the emission spectrum of the fluorescent dye, so that it can deactivate the excited state of these molecules through stimulated emission. The extent of this deactivation depends

[†] Katholieke Universiteit Leuven.
[‡] RIKEN.

(1) Shaner, N. C.; Steinbach, P. A.; Tsien, R. Y. *Nat. Methods* **2005**, *2*, 905−909.
(2) Remington, S. J. *Curr. Opin. Struct. Biol.* **2006**, *16*, 714−721.
(3) Mocz, G. *Mar. Biotechnol.* **2007**, pages 305−328.
(4) Hell, S. W. *Science* **2007**, *316*, 1153−1158.
(5) Hell, S. W. *Opt. Lett.* **1994**, *19*, 780−782.
(6) Klar, T. A.; Hell, S. W. *Opt. Lett.* **1999**, *24*, 954−956.
(7) Klar, T. A.; Jakobs, S.; Dyba, M.; Egner, A.; Hell, S. W. *Proc. Natl. Acad. Sci. U.S.A.* **2000**, *97*, 8206−8210.

10.1021/ja076128z CCC: $37.00

on the local irradiation intensity experienced by the molecules, up to a maximum saturation intensity where the deactivation is essentially complete. Increasing the intensity beyond the saturation intensity does not deactivate more molecules at this location, though it does mean that one can deplete the excited state completely anywhere the donut mode has a nonzero intensity by increasing the total irradiation power. In practice one can do this at any point close to the focus, except at the center, where the intensity is zero. Hence, even though the donut mode is diffraction-limited in itself the saturation allows us to reduce the molecules that remain in the excited state to a spot of subdiffraction dimensions. Because the combination of the excitation and donut-mode depletion beam effectively sets the probability that fluorescence emission may take place at a given coordinate, this method of improving the resolution works regardless of the actual number of dye molecules present.

In principle the concepts behind STED microscopy are not limited to stimulated emission. Indeed, any transition that leads to a loss of fluorescence after photoirradiation can be used, subject to the constraints that this transition should be saturable (i.e., complete) and reversible. The idea of making use of these transitions to obtain a resolution better than the diffraction limit is known as RESOLFT (reversible saturable optical fluorescence transitions) microscopy,[4,8] and suitable candidates for these transitions are the formation of transient "dark" states, such as long-lived triplet states, or the use of fluorescence photoswitching, which is the controlled and reversible on/off switching of the fluorescence emission of a single molecule or construct molecule through photoirradiation. In essence a fluorescence photoswitch can exist in at least two thermally stable states B and A, where state B is fluorescent and state A is essentially nonfluorescent. Through irradiation at a wavelength λ_{BA} or λ_{AB}, respectively, the fluorophore is converted from B to A and vice versa. This switching can be characterized by its efficiency, which is a measure of the speed with which the molecule responds to the applied irradiation, by its fatigue resistance, which determines the amount of switching cycles the molecule can undergo before degradation occurs, and by its thermal stability, which is determined by the rate at which the molecule transitions to the more thermodynamically stable state in the absence of irradiation. To reduce the possibility of unwanted conversion λ_{BA} and λ_{AB} should be well-separated spectrally.

Because of the ease and selectivity allowed by controlling material properties through photoirradiation, considerable research efforts have focused on the discovery and engineering of suitable photoswitches, including fluorescent photoswitches.[9−13] A relatively recent discovery was that of the fluorescent protein Dronpa,[14] which displays fast and reversible photoswitching of its fluorescence emission.[15−17] In several investigations, both at the ensemble and at the single-molecule level, it was shown that the chromophore of Dronpa can exist in at least two stable forms, one of which is brightly fluorescent (state B, $\epsilon = 95\,000$ M^{-1} cm^{-1} at 503 nm, $\phi_{fl} = 0.85$), while the other form is essentially nonfluorescent (state A, $\epsilon = 22\,000$ M^{-1} cm^{-1} at 390 nm, $\phi_{fl} < 0.02$). Based on the pH-dependence of the absorption spectra the fluorescent form (B) and nonfluorescent form (A) are thought to correspond to protonated and deprotonated forms of the chromophore, respectively, and evidence for excited-state proton transfer (ESPT) occurring during the back photoconversion has been uncovered.[18] The possibility of an accompanying cis/trans isomerization has also been proposed.[19] While the actual photophysical scheme is more complicated, involving at least one more protonated dark state,[15] this additional complexity is not directly relevant to this work. Furthermore, several new and promising mutants have been developed that show an increased photoswitching efficiency.[19,20]

In this study we investigate the applicability of thermally stable fluorescence photoswitching in a RESOLFT-like approach for subdiffraction imaging in combination with "donut modes". We pay particular attention to the effects that the photophysical parameters of the photoswitchable fluorophore have on the expected resolution improvement, and to this end we develop a series of numerical calculations which allow us insight into the expected resolution improvement for a particular dye. We experimentally demonstrate the validity of the experimental scheme using a Dronpa mutant called Dronpa-2 (Dronpa Met159Thr).[20]

2. Methods

2.1. Principles of Photoswitching Imaging. Most strategies that have been proposed so far to achieve a diffraction-unlimited resolution in fluorescence microscopy rely on special properties of the labeling fluorophore, including the formation of transient dark states[21−23] or (reversible) photoactivation or photoswitching.[24−29] In this paper we wish to apply the Dronpa photoswitching in combination with a donut-mode beam to achieve a diffraction-unlimited imaging resolution. This technique is conceptually similar to the STED microscopy outlined in the introduction, and a possible scheme to exploit this photoswitching in a RESOLFT-like approach is detailed in Figure 1. Due to the specifics of the photoswitching process three distinct measurement phases are required in the implementation: (i) deactivation of the molecules at the outer edge of the focal volume through irradiation with a donut mode at λ_{BA}, inducing a transition to the photoswitched dark state; (ii)

(8) Hell, S. W. *Nat. Biotechnol.* **2003**, *21*, 1347−1355.
(9) Fukaminato, T.; Sasaki, T.; Kawai, T.; Tamai, N.; Irie, M. *J. Am. Chem. Soc.* **2004**, *126*, 14843−14849.
(10) Matsuda, K.; Irie, M. *J. Photochem. Photobiol. C* **2004**, 169−182.
(11) Heilemann, M.; Margeat, E.; Kasper, R.; Sauer, M.; Tinnefeld, P. *J. Am. Chem. Soc.* **2005**, *127*, 3801−3806.
(12) Lukyanov, K. A.; Chudakov, D. M.; Lukyanov, S.; Verkhusha, V. V. *Nat. Rev. Mol. Cell. Biol.* **2005**, *6*, 885−891.
(13) Bossi, M.; Belov, V.; Polyakova, S.; Hell, S. W. *Angew. Chem., Int. Ed.* **2006**, *45*, 7462−7465.
(14) Ando, R.; Mizuno, H.; Miyawaki, A. *Science* **2004**, *306*, 1370−1373.
(15) Habuchi, S.; Ando, R.; Dedecker, P.; Verheijen, W.; Mizuno, H.; Miyawaki, A.; Hofkens, J. *Proc. Natl. Acad. Sci. U.S.A.* **2005**, *102*, 9511−9516.
(16) Habuchi, S.; Dedecker, P.; Hotta, J.; Flors, C.; Ando, R.; Mizuno, H.; Miyawaki, A.; Hofkens, J. *Photochem. Photobiol. Sci.* **2006**, *5*, 567−576.
(17) Dedecker, P.; Hotta, J.; Ando, R.; Miyawaki, A.; Engelborghs, Y.; Hofkens, J. *Biophys. J.* **2006**, *91*, L45−L47.
(18) Fron, E.; Flors, C.; Schweitzer, G.; Habuchi, S.; Mizuno, H.; Ando, R.; De Schryver, F. C.; Miyawaki, A.; Hofkens, J. *J. Am. Chem. Soc.* **2007**, *129*, 4870−4871.
(19) Stiel, A. C.; Trowitzsch, S.; Weber, G.; Andresen, M.; Eggeling, C.; Hell, S. W.; Jakobs, S.; Wahl, M. C. *Biochem. J.* **2007**, *402*, 35−42.
(20) Ando, R.; Flors, C.; Mizuno, H.; Hofkens, J.; Miyawaki, A. *Biophys. J.* **2007**, *92*, L97−L99.
(21) Enderlein, J. *Appl. Phys. Lett.* **2005**, *87*, 094105.
(22) Gustafsson, M. G. L. *Proc. Natl. Acad. Sci. U.S.A.* **2005**, *102*, 13081−13086.
(23) Bretschneider, S.; Eggeling, C.; Hell, S. W. *Phys. Rev. Lett.* **2007**, *98*, 218103.
(24) Hofmann, M.; Eggeling, C.; Jakobs, S.; Hell, S. W. *Proc. Natl. Acad. Sci. U.S.A.* **2005**, *102*, 17565−17569.
(25) Betzig, E.; Patterson, G. H.; Sougrat, R.; Lindwasser, O. W.; Olenych, S.; Bonifacino, J. S.; Davidson, M.; Lippincott-Schwartz, W. J.; Hess, H. F. *Science* **2006**, *313*, 1642−1645.
(26) Rust, M. J. R.; Bates, M. B.; Zhuang, X. Z. *Nat. Methods* **2006**, *3*, 793−796.
(27) Bossi, M.; Folling, J.; Dyba, M.; Westphal, V.; Hell, S. W. *New J. Phys.* **2006**, *8*, 275.
(28) Schwentker, M. A.; Bock, H.; Hofmann, M.; Jakobs, S.; Bewersdorf, J.; Eggeling, C.; Hell, S. W. *Microsc. Res. Tech.* **2007**, *70*, 269−280.
(29) Hess, S. T.; Girirajan, T. P. K.; Mason, M. D. *Biophys. J.* **2007**, *91*, 4258−4272.

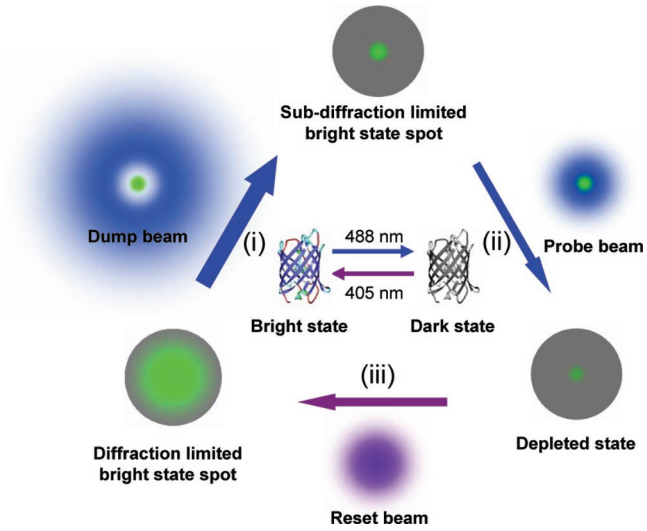

Figure 1. A schematic overview of the measurement. The photoswitchable molecules are initially in the fluorescent state B. By irradiating with the donut mode we selectively switch the molecules that are not at the center of the donut to the photoswitched nonfluorescent state A. The dimensions of the remaining fluorescent region are below the diffraction limit, and by probing the fluorescence with an unmodified (Gaussian) laser beam we can collect fluorescence from this region only. After probing the remaining fluorescence the molecules are reset to the bright state by the reset beam.

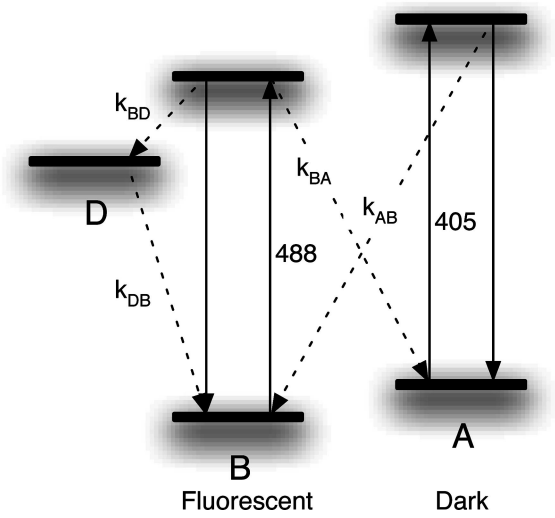

Figure 2. Photophysical scheme used in the calculations: the transitions between the fluorescent (B), photoswitched nonfluorescent (A), and transient nonfluorescent (D) and the associated rate constants are shown by the arrows. Note that k_{BA}, k_{BD}, and k_{AB} take the excitation rates of states B and A into account as well. The dotted lines indicate the possible transitions between the different photophysical states.

probing of the fluorescence emission from the molecules that remain in the bright state by irradiation with a normal-mode laser; and (iii) the recovery of the deactivated molecules to the bright state by irradiation with a laser beam at λ_{AB}, in preparation for the next measurement cycle at a different position on the sample. These phases require three different, overlapping laser beams, which can be conveniently described as "dump", "probe", and "reset", though only the fluorescence generated by the probe beam is collected. A single imaging experiment consists of many such cycles performed in rapid succession at different positions of the sample. While lasers are likely to be the most convenient light source in these measurements any light source providing a sufficiently high irradiance could be used.

The actual resolution improvement is for the most part determined by the depletion in step (i). Moreover, depending on the nature of the photoswitch all three beams can be of different wavelengths, or two of these can be of an identical wavelength. While the Dronpa photoswitching requires only two different wavelengths ($\lambda_{dump} = \lambda_{probe} =$ 488 nm), it is likely that three different wavelengths would be required for a construct molecule (a molecule that consists of two or more different types of chromophores with separate absorption bands, where only one of the chromophores is a photoswitch, e.g., the diarylethene-based photoswitches described in refs 30−32). In this work we will mainly focus on Dronpa-like photoswitches.

2.2. Numerical Simulations. To simulate the effect of the photophysical properties of the fluorophores on the achievable resolution we designed and ran a series of numerical simulations. In these simulations we model the sample as a thin plane containing a large amount of homogeneously distributed photoswitchable molecules, and hence we limit our discussion to the two-dimensional case. However, with a suitable donut-mode beam (i.e., where the intensity zero is confined in all directions) the results for the three-dimensional case should be analogous. We also assume that the photophysics of the sample molecules can be described as three-level systems, consisting of a bright (fluorescent) state B, a photoswitched nonfluorescent state A, and an unknown dark state D which is metastable and is reached through the excitation of the bright state. The overall scheme is summarized in Figure 2, with the possible transitions between the states and the associated rate constants highlighted by the arrows.

For simplicity we further assumed that the transitions between state B and state A and from state B to state D are purely light-induced, that is, not spontaneous, while the transition from D to B is purely spontaneous. Moreover, state A and state B have distinctly separate absorption bands, so that they cannot be excited simultaneously by light of a single wavelength. These requirements are reasonable if we consider only thermally stable and controllable photoswitching, while our modeling of the transitions between B and D is in accordance with the behavior normally observed in single-molecule fluorescence "blinking".[33]

To model the transition rates between the different photophysical levels we assumed that all excitation powers are sufficiently low so that the excitation rates of state A and state B are directly proportional to the intensity of the applied excitation light. Under these circumstances we can model the transition rates from state i to j (k_{ij}) as the product of the excitation intensity (I_{exc}) with the absorption cross section of state i at the used wavelength (σ_i), multiplied by the intrinsic quantum yield of switching from i to j: $k_{ij} = I_{exc} \cdot \sigma_i \cdot \phi_{ij}$. In the simulations we chose to focus on the behavior of Dronpa and Dronpa-2, using parameter values known from ensemble and single-molecule experiments, which are summarized in Table 1.

Because we assume that the sample is densely populated with photoswitchable molecules, our aim is to calculate the fractional populations of each state as a function of time and at different positions on the sample with respect to the focus of the microscope. If all rate constants in the photophysical scheme are known then we can calculate the populations at any instant and starting from an arbitrary set of initial populations (as is detailed in the Supporting Information). Of course, what we are particularly interested in is how the relative populations near the focal region of the microscope evolve during the probe, dump, or reset phase or any sequence of those. We address this issue by calculating the intensity profiles of the laser beams at the focus point using the vector-wave optical theory as developed by Richards and

(30) Irie, M. *Chem. Rev.* **2000**, *100*, 1685−1716.
(31) Irie, M.; Fukaminato, T.; Sasaki, T.; Tamai, N.; Kawai, T. *Nature* **2002**, *420*, 759−760.
(32) Fukaminato, T.; Umemoto, T.; Iwata, Y.; Yokojima, S.; Yoneyama, M.; Nakamura, S.; Irie, M. *J. Am. Chem. Soc.* **2007**, *129*, 5932−5938.
(33) Kohn, F.; Hofkens, J.; Gronheid, R.; Van der Auweraer, M.; De Schryver, F. C. *J. Phys. Chem. A* **2002**, *106*, 4808−4814.
(34) Flors, C.; Hotta, J.; Uji-i, H.; Dedecker, P.; Ando, R.; Mizuno, H.; Miyawaki, A.; Hofkens, J. *J. Am. Chem. Soc.* **2007**, *129*, 13970−13977.

Table 1. Photophysical Parameters used in the Simulations, Based on the Values Determined for Dronpa and Dronpa-2[14,15,34] *a*

	Dronpa	Dronpa-2
σ_{488}	2.21×10^{-16} cm^2	2.14×10^{-16} cm^2
σ_{405}	8.41×10^{-17} cm^2	6.31×10^{-17} cm^2
ϕ_{BA}	3.2×10^{-4}	1.5×10^{-3}
ϕ_{BD}	1.7×10^{-4}	1.35×10^{-2}
ϕ_{AB}	0.37	0.37
$1/k_{DB}$	65 ms	11 ms

[a] Note that the value for ϕ_{BA} for Dronpa-2 differs from the value reported in ref 20. However, we found that in a polyvinyl alcohol (PVA) film Dronpa-2 switches roughly 5 times faster to the dark state compared to Dronpa.

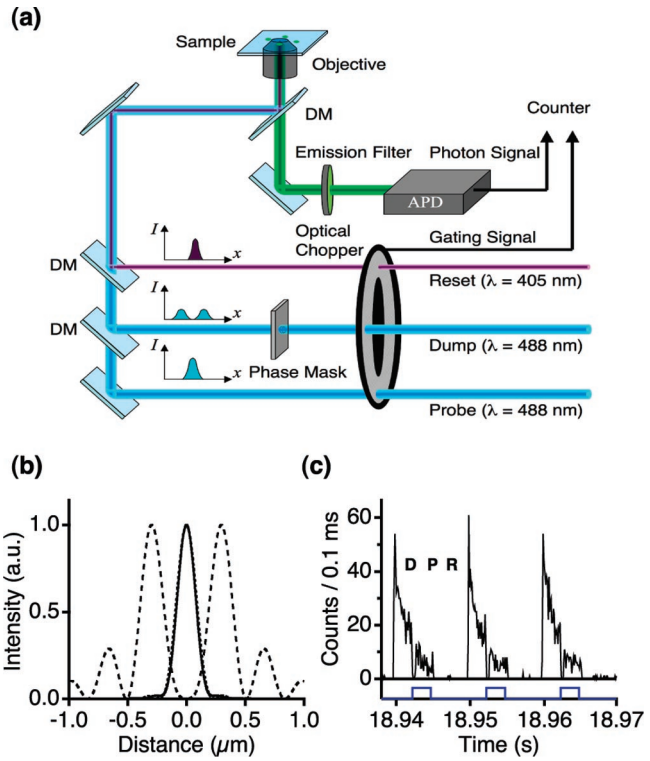

Figure 3. (a) Experimental setup used for the measurements described in this paper. A sample containing Dronpa or Dronpa-2 is sequentially irradiated with a donut-mode beam at 488 nm, followed by the Gaussian-mode probe beam at 488 nm and finally with the reset beam at 405 nm. A mechanical chopper is used to ensure that the beams are introduced in the correct dump−probe−reset sequence and do not overlap in time. (b) The calculated beam profiles for the dump (dashes), probe (dots), and reset (solid) beams. Note that the profiles of the probe and reset beams are very similar. (c) A fluorescence intensity trajectory showing the dump−probe−reset sequence. The actual detection is gated such that only the fluorescence from the probe beam is collected (as shown by the blue trace). For the purpose of clarity the fluorescence depletion due to the dump beam is lower in this figure than what would be required to achieve a sizeable increase in resolution.

Wolf[35,36] (Figure 3b). Inspired by the Dronpa photoswitching we assumed excitation wavelengths of 488 and 405 nm, in combination with a microscope objective with a numerical aperture of 1.3. The calculated excitation profiles for each phase are given in Figure 3b.

With these profiles we can determine the local irradiation intensities at each position with respect to the microscope focus, and thus all of the resulting rate constants are known as well. Hence, by combining the excitation profiles with the photophysical scheme we were able to determine the spatial distribution of the bright state for any arbitrary combination of dump, probe, and reset phases. Moreover, by modeling the spatial depletion of the bright state through the donut-mode illumination we could quantify the expected imaging resolution.

A typical calculation consisted of a single dump−probe cycle, with variable intensities and durations for each phase. For reasons that are explained in the text we generally did not involve the reset phase into the calculations. Because we only collect the fluorescence generated using the probe beam the resolution is only calculated and retained for that phase. Moreover, because the fluorescence readout also affects the bright-state population, the values for the resolution reported in this paper are the intensity-weighted average values over the entire duration of the probe phase.

The details of the calculations used in the simulation are given in the Supporting Information.

2.3. Photoswitching Imaging on Dronpa. The layered double hydroxide (LDH) crystals were prepared using a method described by Oh et al.[37] First, a clear metal solution with 88 mM Mg^{2+} and 44 mM Al^{3+} was prepared by dissolving their nitrate salts in MilliQ (MQ) water. A concentrated NaOH solution (2 M) was added dropwise under vigorous stirring to give a final pH of 11. The resulting mixture was hydrothermally aged in a closed recipient at 80 °C during 12 h, followed by three washing steps with MQ water. A 1 mg amount of the resulting LDH powder was redissolved in 1 mL of MQ water to which 100 μl of a concentrated Dronpa or Dronpa-2 solution (approximately 4 μg/mL) was added. The resulting mixture was stored overnight in a fridge during which the Dronpa proteins adsorbed on the LDH surface. These crystals have been used successfully as substrates for enzyme molecules, demonstrating that the strong electrostatic interactions involved in the adsorption do not necessarily deform the native structure of the protein. After centrifugation the Dronpa-containing LDH crystals could be separated from the clear solution. To prepare the measurement samples 100 μL of the Dronpa−LDH solution was mixed with 100 μL of an MQ solution containing 1 wt % polyvinyl alcohol (PVA). The resulting solution was then spincoated onto carefully cleaned coverglasses at 2000 rpm for 60 s.

The used experimental setup is given in Figure 3a. In brief, the 488 nm line of an Ar/Kr laser (Stabilite 2018-RM, Spectra Physics) was split into two beams with a 50/50 beam splitter. One of these beams was passed through a circular phase mask, which was specially prepared to lead to a "donut mode" upon focusing by the objective,[38] while the other beam was not modified. The 405 nm light was produced by a diode laser (Compass 405, Coherent). All three beams were passed through an optical chopper and were overlapped using dichroic mirrors before entering the Olympus IX-70 confocal microscope equipped with an piezo-scanning stage (PI-517.2CL, Physike Instrumente) and an Olympus UPlanFL N 100 × NA 1.3 objective. The overlap of the three beams was verified to be within 20 nm. The chopper was placed in such a way that the rotation led to the separate introduction of all three beams in the proper dump−probe−reset sequence, with each beam being introduced for 2.5 ms. Introducing the chopper makes it possible to use continuously irradiating lasers in the measurement, and the power of the dump, probe, and reset beams at the sample was 2 μW, 70 nW, and 10 nW, respectively. The beam responsible for the donut mode was additionally passed through a single-mode fiber to ensure that any distortion from the chopper was removed before passing on to the phase mask. The optical chopper used in our experiments, while convenient and relatively inexpensive, limited us to identical durations for the dump, reset, and probe beam. In practice it might be advantageous to use a longer duration for the dump phase compared to the probe phase, and hence we lifted this restriction in the numerical simulations.

The resulting fluorescence emission for all three beams was detected by an avalanche photodiode (SPCM-AQR-14, Perkin-Elmer). The gating of the detection was achieved by only recording those photons that arrived during the probe beam irradiation, by making use of a

(35) Wolf, E. *Proc. R. Soc. London, Ser. A* **1959**, *253*, 349−357.
(36) Richards, B.; Wolf, E. *Proc. R. Soc. London, Ser. A* **1959**, *253*, 358−379.
(37) Oh, J.-M.; Hwang, S.-H.; Choy, J.-H. *Solid State Ion.* **2002**, *151*, 285−291.
(38) Hotta, J.; Uji-i, H.; Hofkens, J. *Opt. Express* **2006**, *14*, 6273−6278.

synchronization signal provided by the optical chopper. The recording of the intensity images and intensity trajectories was done using a counter board (NI PCI-6602, National Instruments) and a single-photon counting computer card (SPC-630, Becker & Hickl), respectively.

Processing of the acquired images was performed using the Matlab software package (Mathworks, Inc.). Similar to the case in ref 24 both the confocal and the high-resolution image were restored by applying two-dimensional image deconvolution using the Richardson−Lucy algorithm with the corresponding calculated PSFs. Prior to the deconvolution process the noise on the images was reduced by convolving the images with a 3×3 pixel Gaussian mask (the distance between adjacent pixels was roughly 40 nm).

3. Results and Discussion

3.1. Numerical Results. 3.1.1. Effect of the Photoswitching Performance. As was mentioned before, the key principle behind this method is the depletion of the fluorescence in the outlying regions of the sample through irradiation with a "donut mode". A larger depletion will lead to a smaller "hole" at the center and hence a larger potential increase in resolution. As a result the imaging resolution of a particular experiment is normally determined for the most part by the "dump" phase, and less so by the "probe" and "reset" phases, though these will also play a part in the outcome of the experiment.

In principle, in any RESOLFT measurement that makes use of donut modes one can consider two different strategies to increase the fluorescence depletion for a given experiment: increasing the irradiation power (which increases the deactivation rate) or increasing the duration of the dump phase (which causes a larger number of molecules to deactivate for a given irradiation power). Interestingly, it turns out that for most of the nonfluorescent states that can be used in RESOLFT measurements it is not possible to increase the duration of the dump phase arbitrarily. For example, in STED measurements the quenching of the fluorescence through stimulated emission has to take place within a fraction of the excited-state lifetime of the dye (i.e., within hundreds of picoseconds) to avoid spontaneous fluorescence emission from the depletion region. Similarly, in RESOLFT experiments that make use of transitions to transient dark states, such as triplet states, the fluorescence depletion will be opposed by the spontaneous recovery of the bright state. Hence we find that the spontaneous recovery of the fluorescent state imposes upper limits on the useful duration of the dump phase, and even more so on the duration of the probe phase (we will examine the effects of spontaneous recovery to the bright state in more detail in what follows). As a result, beyond a certain limit the only useful strategy to increase the resolution is to increase the irradiation power for the dump pulse, possibly to very high values. For example, the extremely short depletion pulses in STED microscopy can require peak intensities of up to $10^{11}-10^{13}$ W/cm^2.[28] Unfortunately, the resolution gain tends to be related to the square root of the applied intensity,[8] marking a clearly decreasing "return on investment" as the irradiation power is increased. The downside to high irradiation powers is that, apart from possibly requiring more advanced equipment, they tend to accelerate the photobleaching of the fluorescent markers.

By contrast, thermally stable photoswitching implies that the recovery from the deactivated state to the fluorescent state does not occur spontaneously. Hence the duration of the dump, probe, and reset phases can in principle be chosen arbitrarily and independently, ranging from microseconds to seconds or more, while avoiding the counteracting of the depletion through the spontaneous recovery of the fluorescent state entirely. This marks a fundamental difference between the photoswitching-RESOLFT and, for example, STED microscopy or "optical shelving" in transient dark states[23] (though the survival times of dark states such as triplet states can sometimes be extended significantly with suitable dyes and careful treatment of the sample[33]). It also means that, by making use of the photoswitching, it is always possible to increase the imaging resolution by increasing the duration of the dump phase, even if the power for the dump irradiation remains unchanged. This finding is confirmed in Figure 4, where we plot the expected resolution as a function of the duration and power of the dump phase. As is clear from this figure, increasing the duration of the dump phase is equivalent to increasing the irradiation power. For example, at a power of 5 μW and 5 ms duration we obtain an approximate resolution of 194 nm in Figure 4b. By increasing the duration to 10 ms we can obtain a resolution of about 180 nm, which is identical to what we would get if we kept the same duration but increased the dump power to 10 μW. This is reasonable considering that, in the absence of spontaneous recovery, the actual fluorescence depletion is determined only by the total number of photons absorbed by the sample, and not by how these photons are distributed in time (note that we neglected the formation of the transient dark state D in these plots. For an example of what these plots look like with its inclusion, see Figure 6).

This finding has two important consequences: By increasing the duration of the dump phase we can get away with arbitrarily low irradiation powers, hence avoiding photobleaching or

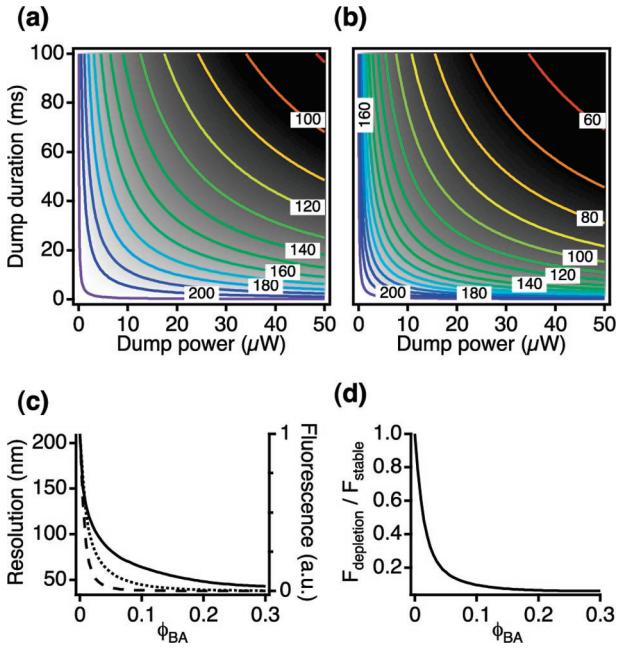

Figure 4. Expected resolution in nanometer as a function of the power and duration of the dump pulse, using the parameters for Dronpa (a) and Dronpa-2 (b). The spacing between the contour lines is 10 nm. In these calculations we assumed that there is no formation of the additional dark state D ($\phi_{BD} = 0$). (c) The estimated resolution (solid line) and fluorescence brightness ($F_{depletion}$, dashed line) as a function of the photoswitching quantum yield ϕ_{BA}. The dotted line denotes the fluorescence brightness (F_{stable}) that would be observed if there was no additional fluorescence depletion during the probe phase. (d) A plot of the ratio $F_{depletion}/F_{stable}$ as function of ϕ_{BA}.

photodegradation, while still obtaining the same spatial resolution (though not time resolution). Second, by increasing both the duration and the irradiation power simultaneously we can improve the resolution more readily. To illustrate this one can see that the contour lines in Figure 4a and b are crossed more easily by moving diagonally on the plot, instead of limiting ourselves to adjusting only the power or the duration (that is, adjusting only in the x or y direction). However, there is a practical limit to the duration of any measurement, and in an actual measurement the acquisition time for measuring a single data point (i.e., a single dump-probe-reset cycle) should be less than 1 s, and preferably even less than 100 ms. This can be due to, for example, mechanical or sample instability, or due to a desire to follow a dynamic process. As a side effect, however, this limitation also clarifies the meaning of "thermally stable" photoswitching. In the context of these measurements this term does not imply that the molecule should be stable indefinitely in both of its photoswitching states but rather that it should be stable compared to the duration of a single dump−probe cycle. In effect, a photoswitchable fluorophore can be considered to be stable if the survival time of both the fluorescent and nonfluorescent state is long compared to the duration of a single measurement cycle (i.e., several seconds or more). Both Dronpa and Dronpa-2 meet these requirements: for Dronpa a value of several hours has been reported,[14−16] while Dronpa-2 takes several minutes to recover to the bright state.[20]

A question that arises is whether there is an optimal quantum yield for the fluorescence deactivation, in the sense that it allows one to achieve a higher imaging resolution with comparatively low irradiation intensities or short measurement durations. At this point one has to discriminate depending on whether the photoswitch is a three-band system or a two-band system, i.e., whether we can readout the fluorescence of the photoswitch while avoiding the transition to the nonfluorescent state. If the switching and fluorescence readout are indeed independent then the answer to this question is brief: the quantum yield of switching should be as high as possible to allow for fast and efficient fluorescence depletion with low irradiation powers.

However, in photoswitches that consist of a single fluorophore the switching to the nonfluorescent state can likely not be decoupled from the fluorescence readout. This is because both the off-switching and the fluorescence emission occur from the same excited state and holds for most photoswitchable compounds as well as for Dronpa. The intuitive view is that a high ϕ_{BA} will lead to a highly efficient fluorescence depletion and thus a large increase in resolution. Unfortunately, the actual scenario is rather more complex than it might seem at first sight: because the fluorescence readout and deactivation cannot be separated, the probe beam, no matter how weak, will always deplete the remaining fluorescence to some extent. If ϕ_{BA} is small then this depletion will go unnoticed; however, if it is not then the depletion will reduce the fluorescence collection and will even start to counteract the resolution increase. As such we arrive at a situation where two counteracting processes meet: if ϕ_{BA} is large then the fluorescence depletion during the dump phase will be favorable, but this will be opposed by the switching during the probe phase, leading to a potentially large reduction in fluorescence intensity. In contrast, if ϕ_{BA} is small then the initial depletion will be less favorable, yet the depletion by the probe beam will also be reduced.

To quantify these effects we calculated the resulting resolution improvement and fluorescence intensities for a typical dump−probe cycle as a function of ϕ_{BA} (note that the values given for the resolution are determined as the intensity-weighted averages over the entire duration of the probe phase, which is 2.5 ms in these calculations). The results are plotted in Figure 4c. From this figure we clearly see that an increased ϕ_{BA} quickly leads to an increased resolution, as expected. However, the effect of the depletion becomes readily apparent when we look at the dashed or dotted line in Figure 4c, which is proportional to the total fluorescence emission and decreases sharply as the switching quantum yield (and resolution) increases.

One might of course argue that this reduction in fluorescence intensity is caused by the very nature of the increased spatial resolution and is not indicative of the photoswitching itself. Indeed, a reduction in fluorescence intensity is a direct consequence of any donut-mode based RESOLFT- or STED-like technique that aims to confine the fluorescence. However, in Dronpa-like photoswitches the fluorescence emission is reduced beyond that which is strictly required by the spatial depletion itself due to the additional photoswitching induced by the probe beam. Indeed, for each ϕ_{BA} we can directly compare the fluorescence collection that would be observed if there were no depletion during the probe phase (F_{stable}) with that of the photoswitchable molecule ($F_{depletion}$). This is shown in Figure 4d, where we plot the ratio $F_{depletion}/F_{stable}$. In this plot we see that this additional depletion is very limited at low values for ϕ_{BA} but becomes very significant for higher values. More precisely, for a switching quantum yield ϕ_{BA} of 0.015 we find that the fluorescence collection is already reduced by a factor of 2 beyond the depletion caused by the fluorescence confinement itself.

While the specific details of Figure 4d depend on the total number of photons that are delivered by the probe beam onto the sample, the observed trend in this figure is general. In these calculations we used a probe duration of 2.5 ms at a power of 50 nW, which is a rather conservative estimate. For longer durations and/or higher irradiation powers the point at which the fluorescence level falls to 50% will be for switching quantum yields that are even lower. For the irradiation power this decrease follows a straightforward fashion; e.g., for a probe power of 100 nW and same duration the 50% point is at a quantum yield of 0.0075, while at 200 nW this occurs at a quantum yield of about 0.003 75. Formally the dependence on the measurement duration is more complex, though the results are similar; e.g., doubling the measurement duration to 5 ms while leaving the irradiation power untouched leads to a quantum yield of 0.0075, and so on.

Maintaining an adequate signal level is a challenge for any technique that aims to increase the resolution through spatial confinement of the fluorescence emission. We therefore believe that the loss of an additional 50% of the emission through photoswitching, on top of the spatial confinement, represents an effective upper limit to the switching quantum yield that is still useful for high-resolution measurements. According to our results a suitable guideline is that the quantum yield of switching to the nonfluorescent state should be less than 0.01. Furthermore this limit is applicable to any RESOLFT-type measurement where the survival time of the nonfluorescent state is long compared the duration of the probe phase.

Some photoswitchable fluorescent proteins, such as asFP595,[24,39] display photoswitching that is different compared to Dronpa. In these proteins the *on*-switching occurs concomitant with the fluorescence emission, while the off-switching requires irradiation at a different wavelength. The inherent limitation in using these proteins in a RESOLFT scheme would not be a loss of fluorescence during the probe phase but rather the reduction of the fluorescence confinement that occurs during this phase due to the on-switching. Hence, for such a photoswitch to be suitable in these measurements the quantum yield of switching to the nonfluorescent state should be high enough to ensure an efficient fluorescence depletion during the dump phase, while the quantum yield of switching to the fluorescent state should be sufficiently low.

3.1.2. Effect of Transient Dark State Formation. Transient nonfluorescent states or dark states are well-known to occur in all fluorophores, though these states can vary greatly in their duration, occurrence, and chemical or physical nature. Intuitively they can be thought of "traps" that render the fluorophore nonfluorescent for a variable duration, followed by spontaneous recovery to the fluorescent state. The duration, or survival time, of the resulting off-time can range from microseconds to milliseconds or more and can be characterized by different distributions (e.g., exponential or power-law distributions[40]) depending on its underlying nature.

It is known from previous studies[15,16] that Dronpa shows a transient nonfluorescent state with a survival time of a few tens of milliseconds, and a similar behavior has been observed for Dronpa-2, though with a survival time of about 11 ms.[34] Moreover, the distribution of the resulting off-times has been experimentally shown to be single-exponential in both cases, which is what we have assumed in the simulations. Because these survival times are of the same magnitude compared to the durations of the different phases in the measurement we decided to investigate the impact of these additional nonfluorescent states (state "D" in our photophysical scheme) on a possible resolution improvement.

Quite generally we can observe that if the formation of this state is very slow ($\phi_{BD} \ll \phi_{BA}$) or if the recovery to the fluorescent state is very fast ($k_{DB} \gg k_{BD}$), then its effects are likely to be negligible. If this is not the case, however, then the picture becomes more complex. Intuitively one can see that the observed effects will depend to a large extent on the survival time of this dark state ($\sim 1/k_{DB}$) relative to the duration of a single measurement cycle. Similarly to the above, if this survival time is very short and the quantum yield of formation is sufficiently low (such as for most triplet states with microsecond survival times) then its effects are likely to be small or negligible, as the fluorescence depletion to the photoswitched dark state is only marginally delayed. In contrast, if the survival time of this state is long on the order of the measurement (tens or hundreds of milliseconds or more) then it becomes a direct competitor to the photoswitching, as determined by the ratio of the corresponding quantum yields of formation.

In a way one might even feel that the presence of such a long-lived dark state is beneficial to the measurement: because this dark state does not recover until after the dump−probe cycle it effectively contributes to the fluorescence depletion during the dump phase. Of course, this does come with a downside, due to the fact that these molecules cannot be recovered to the bright state by the reset beam. Hence subsequent measurements close to the same spot (i.e., at the next position of the scanning stage) are likely to suffer from severe depletion during the probe phase and a resulting low fluorescence signal. This can, of course, be compensated for by increasing the duration of the reset phase or by introducing a waiting period between the measurement cycles, though this is likely to increase the measurement duration significantly.

In between these two effects we find a regime where the fluorescence depletion is actively counteracted by the recovery from state D to state B: the molecules that were depleted to state D during the dump phase recover during the probe phase, which results in an effective worsening of the spatial confinement of the fluorescence.

It is clear then that the exact result of the dark state formation is not trivial and depends on the durations of the different phases involved in the measurement. This is depicted in Figure 5, which details the effective intensity-averaged resolution that results under a given set of experimental and sample conditions. We ran the simulation with different combinations of the dump and probe durations (τ_D and τ_P), using the parameters for Dronpa-2, and with the assumptions that the dump and probe powers are 5 μW and 12.5 nW at the sample, respectively. In these plots we can indeed discover the different regimes discussed above, with an initial worsening of the resolution followed by an improvement as the survival time is increased, as the additional fluorescence depletion increasingly dominates the spontaneous recovery of the dark state. This is depicted in more detail in Figure 5e. An increasing quantum yield of formation of the dark state tends to emphasize the effects of the survival time, though for high quantum yields the resolution decreases due to the additional depletion by the probe beam. This figure also shows that the durations of the probe and reset phases have to be taken into account when judging the importance of dark state formation on the measurement.

In conclusion, and as one might expect, we can say that in general the presence of additional dark states should be avoided as much as possible, and not only because they tend to decrease the brightness of the dye and have been suggested to be involved in photobleaching.[41] We find that they mostly tend to counteract the measurements described here. However, based on the simulations we find that the exact effects can vary significantly depending on the quantum yield of formation and the survival time of this dark state and the parameters of the measurement, as can be seen in Figure 5a−d.

3.1.3. Photoswitching Fatigue Resistance and Reset Phase. Obtaining a high imaging resolution requires both extensive fluorescence depletion and sampling points that are sufficiently close together (i.e., we have to conduct the dump−probe−reset cycles at points that are spaced closer together on the sample in order to make effective use of the enhanced resolution). As a result a given molecule will need to undergo an increasing number of switching events as the resolution increases, both due to the need for more aggressive switching and due to the requirement for more extensive sampling. Hence the number

(39) Schäfer, L. V.; Groenhof, G.; Klingen, A. R.; Ullmann, G.; Boggio-Pasqua, M. M.; Robb, M. A.; Grubmüller, H. *Angew. Chem., Int. Ed.* **2007**, *46*, 530−536.

(40) Clifford, J.; Bell, T. D. M.; Tinnefeld, P.; Heilemann, M.; Melnikov, S. M.; Hotta, J.; Sliwa, M.; Dedecker, P.; Sauer, M.; Hofkens, J.; Yeow, E. K. L. *J. Phys. Chem. B* **2007**, *111*, 6987−6991.

(41) Donnert, G.; Eggeling, C.; Hell, S. W. *Nat. Methods* **2007**, *4*, 81−86.

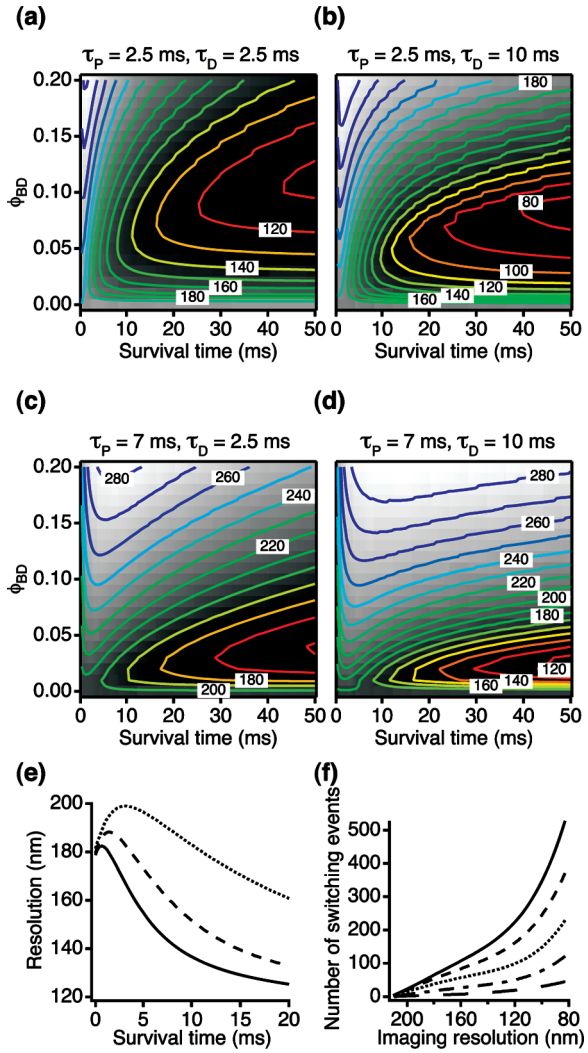

Figure 5. (a−d) Effect of the quantum yield and survival time of the nonfluorescent state D on the expected imaging resolution, for different durations of the probe and reset phase. The spacing between the contour lines is 20 nm. The other parameters used in the calculation are those of Dronpa-2, though the plot is similar for Dronpa. In these calculations we assumed irradiation powers of 5 μW for the dump beam and 12.5 nW for the probe beam. (e) The effect of the survival time of this nonfluorescent state on the resolution for different durations of the probe phase: 2.5 ms (solid line), 5 ms (dashed line), and 10 ms (dotted line). The duration of the dump phase is 10 ms in this plot. (f) The approximate number of switching cycles required for a single molecule as a function of the imaging resolution and for different active radii of the reset phase: (from top to bottom) 600, 500, 400, 300, and 200 nm.

of cycles that the photoswitch can undergo without degradation (the fatigue resistance) has to increase as well to keep up.

One of the major factors in this regard is the amount of molecules that we reactivate with each reset pulse. If we reset a larger area of molecules surrounding the focus point then most of these molecules will have to be deactivated again in the next imaging cycle. The most interesting prospect then is to reset the smallest possible area of the sample, by confining the reset irradiation to the center focus point as much as possible. To illustrate, Figure 5f shows the approximate number of switching cycles that a molecule would ideally have to perform for a given imaging resolution, if the reset irradiation is such that only the molecules within a circular spot with the given diameter surrounding the focus point are reset. In this calculation, which is detailed in the Supporting Information, we assumed that the measurement points on the sample are spaced along a square lattice with sides equal to half the resolution (i.e., for an approximate resolution of 150 nm we assume that the spacing between the lattice points is 75 nm). Moreover we assumed that a single dump−probe−reset cycle is performed at each point.

At higher imaging resolutions the number of switching events increases dramatically. Moreover, for a molecule that is very efficiently recovered to the bright state (such as Dronpa) it can be difficult to confine the reset phase to a small area of the sample, so that there can be tens or hundreds of switching events. While over 100 switching cycles have been reported for a single Dronpa molecule,[15] this is close to, or even above, the limitations that are currently known for single-molecule photoswitching and hence poses a significant problem. In practice, however, a given molecule does not have to respond to all the switching events in Figure 5f. Due to the assumed symmetry of the scanning the molecule will be at the center of the focus after half of these events and will not contribute significantly to the recorded probe emission after a few more cycles. Hence, after about half of these switching events it can bleach safely, without affecting the measurement in a detrimental way (except for rendering the measurement irreversible). Moreover, because the sample should be labeled with a preferably large amount of dyes, some partial photobleaching is acceptable.

As is clear from Figure 5f, we can further try to mitigate the number of required photoswitching cycles by decreasing the active area of the reset phase, in the sense that less molecules are reset to the bright state after each reset pulse. This outlines the ideal scenario that one should take for the reset phase: the reset beam should restore the least amount of molecules possible to the bright state. In this context the meaning of the "least amount of molecules" is rather loose, depending on the desired imaging resolution and on the specifics of the measurement (such as the distance between the sampling points or the scanning speed). As such we do not take the reset phase into account explicitly in our simulations, meaning that we start every simulation from an ensemble of molecules in the bright state.

In general the optimum photophysical parameters for the reverse photoswitching (A to B) depend entirely on how well the absorption bands of the fluorescent and photoswitched nonfluorescent form are separated. Due to our need for efficient fluorescence depletion during the dump phase we require that $k_{BA} \gg k_{AB}$ when we irradiate at λ_{BA}. If state A absorbs essentially no radiation at this wavelength then ϕ_{AB} can be very large; however, if A has a significant absorption then ϕ_{AB} should be small to ensure that this condition can be met.

While it is possible to relax the photoswitching requirements significantly by carefully optimizing the measurement settings, the demands imposed by this measurement on the fatigue resistance of the photoswitching remain a challenge.

3.2. Experimental Results. We felt that the use of Dronpa and Dronpa mutants in these experiments is promising as these proteins are essentially completely thermally stable on the time scale of the measurements, respond quickly to the applied irradiation, and yet should still produce enough photons to be detectable during the probe phase. To this end we prepared several samples containing Dronpa or Dronpa-2 and measured them on the setup shown in Figure 3a. Unfortunately, we found

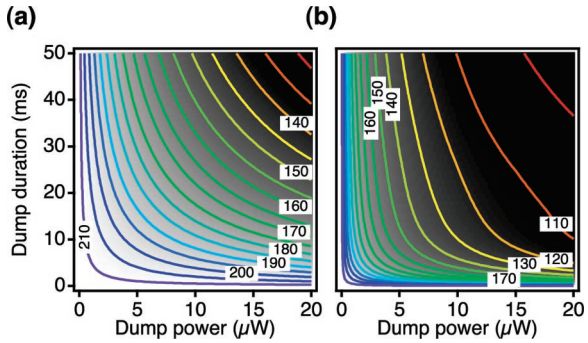

Figure 6. Estimated resolution for Dronpa (a) and Dronpa-2 (b), using the experimental parameters and as a function of the dump power and duration. The asymmetry in (b) is due to the more pronounced presence of the transient dark state D in Dronpa-2 as compared to Dronpa. The spacing between the contour lines is 10 nm.

that the original Dronpa displayed severe photobleaching at irradiation powers of the dump beam over about 1 μW, which is not sufficient to obtain a sizable resolution increase (Figure 6a). While we could improve the photostability somewhat by adjusting the sample preparation, this increase was not sufficient and as a result we did not pursue these measurements further. Fortunately we found Dronpa-2 to be more photostable compared to Dronpa, being able to resist irradiation powers of a few microwatts at the objective without too severe photobleaching (< 50%). Moreover, because the dump power which we could apply was inherently limited by the bleaching we felt that this mutant was more promising due to its larger quantum yield of switching as well as the possibility of forming a long-lived dark state (though Dronpa has an even longer-lived dark state, albeit with a lower quantum yield of formation).

Figure 7 shows some example results obtained on the Dronpa−LDH sample. Figure 7a represents a scanning image recorded for a region of the sample without using the dump beam (i.e., by running the full measurement cycle for each point but while blocking the dump beam), while Figure 7b is a scan of the same area of the sample but with the dump beam as well. By visually inspecting these plots and by constructing line profiles (Figure 7e), we can see a clear difference between the images; however, these differences become more readily apparent after the deconvolution of both of the images (Figure 7c and d). Moreover, the increased resolving power of the system is readily apparent in the resulting line profiles (Figure 7f).

On comparing different line profiles through Figure 7a and b we estimated a resolution improvement of about 18% with the dump beam. The simulations predict a 15% improvement under these sampling conditions, which is in good agreement.

According to Figure 6b it should be possible to increase the resolution further by increasing the duration of the dump irradiation, however, we did not observe a significant increase. This is likely due to the increase in photobleaching that occurs for longer irradiation times. In principle this could be avoided by increasing the irradiation times even further, though because the optical chopper only allows us to change the duration of all three phases simultaneously the total measurement duration would rapidly become very long.

While the use of photoswitching in obtaining an enhanced resolution by making use of "donut modes" has been demonstrated before on a mixture of two types of molecules,[27] we believe that these measurements mark the first time that an

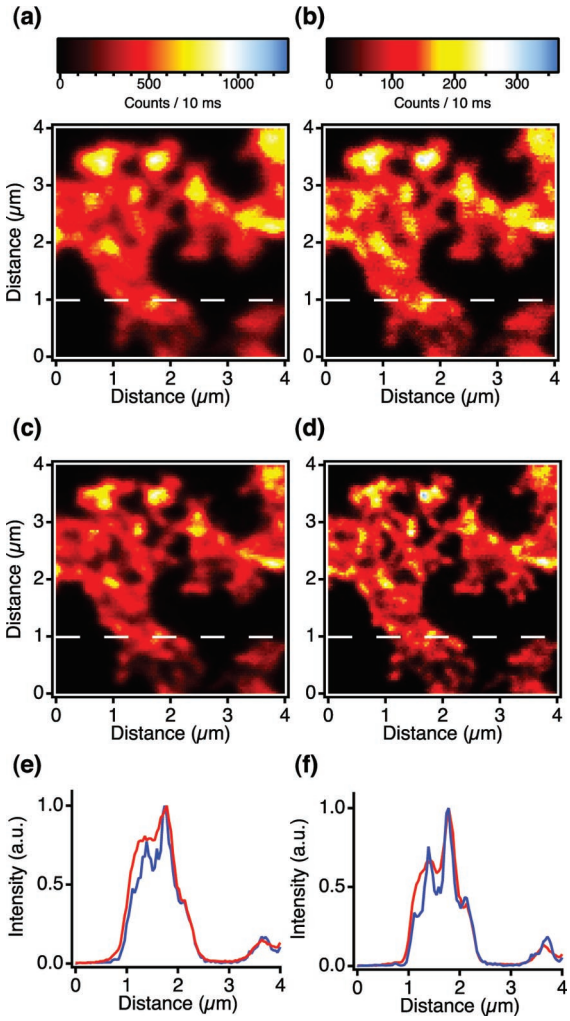

Figure 7. Scanning images of a sample of Dronpa-2 molecules adsorbed on 100 nm crystals in PVA matrix without (a) and with (b) the dump beam. (c−d) The images from (a) and (b) after deconvolution. (e) Measured line profiles through the scanning images in (a) and (b), as indicated by the white dashed line. (f) The same line profiles but through the deconvolved images (c) and (d). The blue and red lines represent the line profiles in the absence (red) and presence (blue) of the dump beam.

increase in resolution has been demonstrated for a thermally stable, Dronpa-like, photoswitchable molecule using a donut-mode approach. At this point, however, we are limited by the rather low photostability of the dye, and new photoswitchable fluorophores will be required before this technique can reach its full potential.

4. Conclusion

In this paper we have focused on the possibility of achieving a subdiffraction resolution by making use of the thermally stable photoswitching of a Dronpa fluorophore in combination with "donut-mode" illumination. To this end we have made a series of simulations with the aim of determining an optimal range of photophysical parameters that are useful in obtaining resolution improvement. We quantify these parameters in terms of a three-level system which we find adequately describes Dronpa and its mutants, enabling us to determine a range of parameters that would render a particular photoswitch a potential candidate for use in these measurements. We limited our work and discussion to photoswitches that display photophysics similar to Dronpa, that is, where fluorescence emission and switching to the

nonfluorescent state are accomplished by irradiating in the same absorption band.

By making use of the thermally stable photoswitching we can avoid very high irradiation powers for the donut beam while still achieving a sizable resolution increase by increasing the duration of the dump pulse. Moreover, if the duration and irradiation power are increased simultaneously then a higher imaging resolution can be achieved more readily, though the results depend on the photophysics of the photoswitchable dye. For this reason we decided to investigate this in more detail using a photophysical scheme that can be applied to many different dyes.

We found that an increased quantum yield of switching to the dark state (ϕ_{BA}) will in general result in an increased resolution, as one can expect intuitively. However, if the quantum yield of switching is too high then the irradiation that is required to probe the residual fluorescence will in itself deplete the fluorescence emission, resulting in a reduced signal-to-noise ratio and a slightly decreased imaging resolution. We find that, in general, a quantum yield below 0.01 is preferable.

The presence of an additional transient dark state D that is formed upon irradiating the bright state is not necessarily detrimental to the measurement. Indeed, the exact impact that this state will have on the measurement depends on its quantum yield of formation (ϕ_{BD}) and on its survival time. Briefly, very short-lived nonfluorescent states, such as most triplet states, will not have a significant impact on the measurement. In contrast, long-lived dark states (tens or hundreds of milliseconds or more) tend to accelerate the fluorescence depletion. Indeed, in this case we have to look at the "effective quantum yield of depletion" $\phi_D = \phi_{BA} + \phi_{BD}$. Similar to the case made above we should ideally have $\phi_D < 0.01$. This additional depletion comes at a cost, however, in the sense that the molecules in state D are not recovered by the reset irradiation, and hence the fluorescence brightness of that part of the sample is decreased until the fluorescent state is spontaneously recovered, potentially hindering subsequent measurement cycles. For survival times that are on the order of the dump and probe duration we find that there is a net counteraction of the depletion, resulting in a worsening of the apparent resolution.

We did not discuss in any detail the effects of the reset irradiation, instead assuming that we could reliably reset the molecules in an area surrounding the focal region to the fluorescent state. If we neglect photobleaching then this is always possible, though the required duration may vary (e.g., the quantum yield of reverse photoswitching could be low, or the nonfluorescent state A could possess a transient dark state). In general, the maximum efficiency (quantum yield) for the on-photoswitching is determined by the overlap between the absorption bands of the fluorescent and the photoswitched nonfluorescent form. If this overlap is small then ϕ_{AB} should be large, while if it is significant ϕ_{AB} should be small. We connected this discussion with that of the required number of switching cycles that a particular molecule has to perform. This number depends on the desired resolution and on the specifics of the measurement setup, ranging from a few tens to over one hundred individual switching events, though these numbers can be reduced by carefully controlling the extent of the reset irradiation.

We then demonstrated the possibility of achieving a resolution increase with this technique by making use of the photoswitching of Dronpa-2. While the actual resolution improvement of these measurements was limited, these limitations are not inherent to the method but are rather determined by the specific properties of Dronpa-2 and, in particular, the limited photostability of this photoswitch. Nevertheless we feel that this technique is promising and that the availability of mutants with an improved photostability or of other photostable and efficient fluorescence photoswitches would enable this method to be used to its full potential.

Subdiffraction imaging relies on exploiting the photophysics of the sample fluorophores to achieve a selective spatial or temporal suppression of the fluorescence. While many of the challenges in these measurements are of a technical nature, the properties of the fluorescent label remain one of the most critical and determining aspects. Indeed, significant challenges remain in the design and synthesis of novel (photoswitchable) fluorescent compounds with improved properties, and we believe that the results published in this work can be used as guidelines to assess the suitability of a prospective dye for this type of measurement.

Acknowledgment. P.D. is a fellow of the Fonds voor Wetenschappelijk Onderzoek (Aspirant van het FWO) and would like to thank S. Vancoillie for stimulating discussions. Support from the FWO (Grant G.0366.06), the KULeuven Research Fund (GOA 2006/2, Center of Exellence INPAC through a postdoctoral fellowship to C. Flors, CREA2007), the Flemish Ministry of Education (ZWAP 04/007), and the Federal Science Policy of Belgium (IAP-VI/27) is gratefully acknowledged. This work, as part of the European Science Foundation EUROCORES Programme SONS, was supported from funds by the FWO and the EC 6th Framework Program (ERAS-CT-2003-980409). This work was partially financed by the Impulse Initiative Cell Imaging Core of the K.U. Leuven (via a fellowship to J.H.). M.R. is funded by a grant from the Institute for the Promotion of Innovation by Science and Technology in Flanders.

Supporting Information Available: Details on the numerical simulations. This material is available free of charge via the Internet at http://pubs.acs.org.

JA076128Z